

PUBLICATION VI

**Effect of the target motion sampling  
temperature treatment method on the  
statistics and performance**

Ann. Nucl. Energy, Accepted for publication Aug 21, 2014.

Copyright 2014 Elsevier Ltd.

Reprinted with permission from the publisher.



Contents lists available at ScienceDirect

## Annals of Nuclear Energy

journal homepage: [www.elsevier.com/locate/anucene](http://www.elsevier.com/locate/anucene)

## Effect of the Target Motion Sampling temperature treatment method on the statistics and performance

Tuomas Viitanen\*, Jaakko Leppänen

VTT Technical Research Centre of Finland, P.O. Box 1000, FI-02044 VTT, Finland

## ARTICLE INFO

## Article history:

Received 22 April 2014

Received in revised form 14 August 2014

Accepted 14 August 2014

Available online xxx

## Keywords:

Monte Carlo

On-the-fly

Temperature

Collision estimator

## ABSTRACT

Target Motion Sampling (TMS) is a stochastic on-the-fly temperature treatment technique that is being developed as a part of the Monte Carlo reactor physics code Serpent. The method provides for modeling of arbitrary temperatures in continuous-energy Monte Carlo tracking routines with only one set of cross sections stored in the computer memory.

Previously, only the performance of the TMS method in terms of CPU time per transported neutron has been discussed. Since the effective cross sections are not calculated at any point of a transport simulation with TMS, reaction rate estimators must be scored using sampled cross sections, which is expected to increase the variances and, consequently, to decrease the figures-of-merit. This paper examines the effects of the TMS on the statistics and performance in practical calculations involving reaction rate estimation with collision estimators.

Against all expectations it turned out that the usage of sampled response values has no practical effect on the performance of reaction rate estimators when using TMS with elevated basis cross section temperatures (EBT), i.e. the usual way. With 0 Kelvin cross sections a significant increase in the variances of capture rate estimators was observed right below the energy region of unresolved resonances, but at these energies the figures-of-merit could be increased using a simple resampling technique to decrease the variances of the responses. It was, however, noticed that the usage of the TMS method increases the statistical deviances of all estimators, including the flux estimator, by tens of percents in the vicinity of very strong resonances. This effect is actually not related to the usage of sampled responses, but is instead an inherent property of the TMS tracking method and concerns both EBT and 0 K calculations.

© 2014 Elsevier Ltd. All rights reserved.

### 1. Introduction

The traditional continuous-energy Monte Carlo tracking approach relies on effective cross sections. In other words, the cross sections are Doppler-broadened to match the temperatures of the transport problem beforehand and used as-is throughout the transport simulation. Since cross sections for each nuclide and temperature must be stored separately in the computer memory, the memory requirement of the pre-broadened cross sections may increase to an intolerable magnitude. Particularly, the computer memory becomes a significant limitation when modeling systems with numerous nuclides and temperatures, as is often the case in multi-physics applications of Monte Carlo. To get rid of the memory limitation and, thus, to provide for modeling of systems with complex temperature distributions, on-the-fly temperature treatment techniques are required.

This article discusses a promising on-the-fly temperature treatment technique, in which the effective cross sections are not calculated at any point, but the thermal motion of target nuclei is handled stochastically by sampling target velocities at each collision site. With this approach, only one set of continuous-energy cross sections needs to be stored in the computer memory regardless of the number of temperatures appearing in the system. As a novel feature, the Target Motion Sampling (TMS) temperature treatment method only sees the temperature through an arbitrary variable  $T(\mathbf{r}, t)$ , which may vary continuously in both space and time. The capability to easily model realistic temperature distributions makes TMS a very attractive temperature treatment technique to be used in multi-physics couplings.

The idea behind this technique was introduced for the first time in English-written journals by the authors in Viitanen and Leppänen (2012b) and it was implemented in the Monte Carlo reactor physics code Serpent<sup>1</sup> shortly afterwards (Viitanen and

\* Corresponding author. Tel.: +358 40 763 1963; fax: +358 20 722 5000.

E-mail address: [tuomas.viitanen@vtt.fi](mailto:tuomas.viitanen@vtt.fi) (T. Viitanen).

<sup>1</sup> A complete and up-to-date description of the Serpent code is found at the project website: <http://montecarlo.vtt.fi>

Leppänen, 2012a). It was, however, recently learned that a technique similar to TMS has been introduced in a Russian journal already in the 1980s (Ogibin and Orlov, 1984). The development of the TMS method is still on-going, and recently the main focus in the development has been on the optimization of the method (Viitanen and Leppänen, 2013, 2014). Near-future challenges in the development involve at least the extension of the method to the energy range of unresolved resonances and the application of the method together with  $S(\alpha, \beta)$  tables for bound-atom scattering.

This work concentrates on an anticipated challenge related to the reaction rate estimators: since the effective cross sections are not available during the transport simulation when tracking with the TMS method, the reaction rate estimators need to be scored using sampled cross sections. As the scores become distributed quantities, the variances of the estimators may increase significantly. On the other hand, the usage of the TMS increases the total number of collisions in a calculation, which has an opposite effect on the variances of collision estimators when considering a constant number of neutron histories. Hence, the total effect of the TMS method on estimator deviances is hard to figure out without testing it in practice.

The effect of the TMS method on statistics and performance of reaction rate estimators is studied in the current work. First, an introduction to the TMS method and reaction rate estimators are provided in Sections 2 and 3, respectively. Four realistic fuel assemblies, used to test the estimators in practice, are presented shortly in Section 4 and selected results of the calculations are provided in Section 5. The last Section 6 is dedicated for summary and conclusions.

## 2. Target Motion Sampling (TMS) temperature treatment

The TMS temperature treatment technique is basically a tracking scheme that takes the effect of thermal motion into account during the tracking simulation (Viitanen and Leppänen, 2012b, 2014). The neutron path lengths are sampled based on a “temperature majorant” cross section

$$\Sigma_{\text{maj}}(E) = \sum_i \Sigma_{\text{maj},i}(E) = \sum_i g_i(E, \Delta T_i) \max_{E' \in [E_{\text{min}}, E_{\text{max}}]} \Sigma_{\text{tot},i}(E', T_{\text{base}}), \quad (1)$$

where  $E$  is the neutron energy,  $T_{\text{max},i}$  is the maximum temperature of nuclide  $i$ ,  $\Sigma_{\text{tot},i}$  is the macroscopic total cross section of nuclide  $i$ ,  $T_{\text{base}}$  is the basis temperature of the cross section and  $[E_{\text{min}}, E_{\text{max}}]$  is the energy range of thermal motion around  $E$ , which corresponds to the temperature difference

$$\Delta T_i = T_{\text{max},i} - T_{\text{base},i}. \quad (2)$$

The  $g_i$  factor in Eq. (1) is the Doppler-broadening integral for constant cross section

$$g_i(E, \Delta T) = \left( 1 + \frac{1}{2\lambda(\Delta T, A_i)^2 E} \right) \text{erf} \left( \lambda(\Delta T, A_i) \sqrt{E} \right) + \frac{e^{-\lambda(\Delta T, A_i)^2 E}}{\sqrt{\pi} \lambda(\Delta T, A_i) \sqrt{E}}, \quad (3)$$

where  $A_i$  is the atomic weight ratio of nuclide  $i$ ,

$$\lambda(\Delta T, A) = \sqrt{\frac{A}{k_B \Delta T}} \quad (4)$$

and  $k_B$  is the Boltzmann constant (X-5 Monte Carlo Team, 2003).

The energy range of the thermal motion depends on the mass of the target nuclide and the neutron energy  $E$  in addition to  $\Delta T$ . In the current Serpent version, the energy boundaries are chosen

similar to the elastic scattering majorant of the Doppler-broadening rejection correction (DBRC) method<sup>2</sup> (Becker et al., 2009). Thus, the minimum energy in the range is

$$E_{\text{min}}(E, \Delta T_i, A_i) = \left( \sqrt{E} - \frac{4}{\lambda(\Delta T, A_i)} \right)^2 \quad (5)$$

and the maximum energy is

$$E_{\text{max}}(E, \Delta T_i, A_i) = \left( \sqrt{E} + \frac{4}{\lambda(\Delta T, A_i)} \right)^2. \quad (6)$$

From (5) and (6) it is also easy to derive a formula for the width of the energy range:

$$E_{\text{max}} - E_{\text{min}} = 16 \frac{\sqrt{E}}{\lambda(\Delta T, A_i)} = 16 \sqrt{\frac{E k_B \Delta T}{A_i}}. \quad (7)$$

The path length  $l$  and, thus, the next collision point candidate are obtained using inversion sampling

$$l = -\frac{1}{\Sigma_{\text{maj}}(E)} \ln(\xi), \quad (8)$$

where  $\xi$  is a uniformly distributed random variable on the unit interval. At the collision point, the target nuclide candidate is first sampled such that the probability of sampling nuclide  $i$  is simply

$$P_i = \frac{\Sigma_{\text{maj},i}(E)}{\Sigma_{\text{maj}}(E)}. \quad (9)$$

Then, the target velocity  $V_t$  and cosine between the directions of the target and neutron  $\mu$  are sampled from the distribution

$$P(V_t, \mu, T - T_{\text{base}}, A_i) = \frac{v'}{2v} P_{\text{MB}}(V_t, T - T_{\text{base}}, A_i), \quad (10)$$

where  $T$  is the local temperature at the collision point,  $v$  is the LAB-frame speed of the neutron and

$$v' = \sqrt{v^2 + V_t^2 - 2vV_t\mu} \quad (11)$$

is the relative speed of the neutron to the target (target-at-rest velocity). Symbol  $P_{\text{MB}}$  stands for the Maxwell–Boltzmann distribution for the target speed, defined

$$P_{\text{MB}}(V_t, T, A) = \frac{4}{\sqrt{\pi}} \gamma(T, A)^3 V_t^2 e^{-\gamma(T, A)^2 V_t^2}, \quad (12)$$

where

$$\gamma(T, A) = \sqrt{\frac{AM_n}{2k_B T}} \quad (13)$$

and  $M_n$  is the neutron mass.

The collision point is accepted or rejected according to the rejection sampling criterion

$$\xi < \frac{g_i(E, T - T_{\text{base}}) \Sigma_{\text{tot},i}(E', T_{\text{base}})}{\Sigma_{\text{maj},i}(E)}, \quad (14)$$

where  $E'$  is the target-at-rest energy corresponding to speed  $v'$ . In case the collision is rejected, the tracking proceeds by sampling of a new path length beginning from the current collision point candidate. If the collision is accepted, a reaction is sampled using the cross sections at temperature  $T_{\text{base}}$  such that the probability of sampling reaction  $j$  is

<sup>2</sup> Previous results, published in Viitanen and Leppänen (2013), have shown that the energy boundaries could be chosen in a more efficient way, leading to better performance without compromising the accuracy of the calculations in practice. However, the final implementation of this optimization technique is still incomplete and, therefore, the less efficient DBRC boundaries will have to do for now.

$$P_j = \frac{\Sigma_{ij}(E', T_{\text{base}})}{\Sigma_{\text{tot},i}(E', T_{\text{base}})}. \quad (15)$$

The tracking procedure continues according to the sampled reaction.

It has been shown in Viitanen and Leppänen (2012b) that this tracking scheme, with  $T_{\text{base}} = 0\text{K}$ , reproduces the same mean free paths and reaction rates as conventional tracking methods relying on effective, pre-broadened cross sections. The elevating of the basis cross section temperature has been further discussed in Viitanen and Leppänen (2014), where the functionality and feasibility of the TMS technique with  $T_{\text{base}} \geq 0\text{K}$  have been demonstrated in four realistic systems with different characteristics.

### 3. Reaction rate estimators

#### 3.1. Track-length estimators

The basic idea behind the track-length estimators is that the volume-integrated neutron flux, by definition, equals the total track-length of neutrons. Hence, the neutron track-lengths can be used to estimate the total neutron flux. The track-length estimators are scored every time a neutron draws a track in the volume of interest, i.e. the cell, universe or material in which the reaction rates are calculated. The scores are defined

$$s = fw l_t, \quad (16)$$

where  $w$  is the weight of the neutron,  $l_t$  is the track length of the neutron in the volume of interest and  $f$  is the response, which is chosen according to the reaction rate being calculated. For example,  $f = 1$  would be used to calculate the total neutron flux,  $f = \Sigma_{\text{tot}}(E, T)$  to calculate the total reaction rate and  $f = \Sigma_{\gamma,i}(E, T)$  to calculate the radiative capture reaction rate of nuclide  $i$ . The scores can be binned with respect of different variables, most commonly energy. For instance, by storing separately the scores for  $E \leq 1\text{eV}$  and  $E > 1\text{eV}$  it is possible to separate the reactions induced by thermal and fast neutrons from each other (Lux and Koblinger, 1990).

The usage of the track-length estimator is limited by two facts:

1. The track-length estimator involves an assumption that the cross section response used in the scoring (Eq. (16)) represents the whole track length  $l_t$ . Consequently, the volume in which the estimator is scored must be homogeneous in terms of nuclide composition, density and temperature when using cross sections as responses.
2. The track-lengths  $l_t$  within the volume of interest must be resolvable.

Because of the first limitation, the track-length estimators are not very well suited with the TMS method. Usage of track-length estimators would prevent the modeling of continuous temperature distributions within material zones, thus vitiating a major advantage of the TMS method. The second limitation is only related to the geometry routine of Serpent, which combines surface-tracking with the Woodcock delta-tracking method (Leppänen, 2010). Since the surface crossings are not recorded with the Woodcock delta-tracking, the track-lengths cannot be resolved without significant extra effort and, thus, the track-length estimators cannot be scored in practice. For this reason, the track-length estimator has not been implemented in Serpent 2 and track-length estimators are not used in the current article.<sup>3</sup>

<sup>3</sup> The functionality of the TMS method together with track-length estimators has not been demonstrated, either.

#### 3.2. Collision estimators

Collision estimators are based on the simulated total reaction rates. As the reaction rate of a partial reaction is related to the total reaction rate simply by the ratio of its cross section to the total cross section, the collision estimators of any reactions can be scored every time a reaction takes place in the neutron transport (Lux and Koblinger, 1990).

With the TMS method, the collision estimators are scored at each collision site, regardless of whether the collision point is accepted or not. The scored values can be written as

$$s = \frac{fw}{\Sigma_{\text{maj}}(E)}, \quad (17)$$

where  $f$  is the value of the response and  $\Sigma_{\text{maj}}$  is the material-wise TMS majorant cross section.

Again, the effective cross sections are not available in TMS transport and the temperature dependence of the responses must be handled in a different way (Section 3.3). Unlike track-length estimators, collision estimators can be used to score reaction rates in material zones with inhomogeneous temperature distributions. Therefore, they are the natural choice to be used with the TMS temperature treatment technique. All the reaction rates in this article are calculated using collision estimators.

#### 3.3. Distributed responses

One challenge in the scoring of reaction rate estimators is that the effective cross sections used as responses  $f$  are, in general, not available at the desired temperature when using the TMS temperature treatment. With track-length estimators the response should be in the homogeneous temperature of the surrounding material, while the local temperature  $T$  of the collision point should be used in the scoring of the collision estimators.

The issue is very similar to the basic problem of on-the-fly temperature treatment in Monte Carlo neutron transport—and so is its solution. Analogous to the TMS approach in neutron transport, a cross section in  $T_{\text{base}}$  temperature corresponding to a target-at-rest energy sampled from Eq. (10) is used. Furthermore the responses must be multiplied with the Doppler-broadening integral for constant cross section, Eq. (3). When scored this way, i.e. using responses

$$f = g_i(E, T - T_{\text{base}}) \Sigma_x(E', T_{\text{base}}), \quad (18)$$

the expectation values of the reaction rate estimators are not affected since the sampled cross sections correspond to the effective cross section on average. However, the variances of the estimators increase because the responses become distributed quantities. The variance of the response  $f$  depends on the temperature difference between the response and  $T_{\text{base}}$ : the larger the difference, the wider the distribution of  $E'$  and, thus, the larger the variance of  $\Sigma_x(E', T_{\text{base}})$ .

In the current implementation of the TMS method in Serpent, the implicit estimator of  $k_{\text{eff}}$  is automatically scored at each collision point. Since the scoring involves calculation of several reaction rates, the velocities of all nuclei in the collision material are always sampled for each collision and the same velocities can be used when scoring reaction rate estimators. Consequently, the extra CPU time spent in the scoring of reaction rate estimators in the current implementation is somewhat smaller than if the target velocities would be sampled separately while scoring the estimators.

It is easy to figure out a variance reduction technique for the responses (18). Instead of using a single sample for the response, one may decrease the variance of the response by using an average of  $N$  sampled values,

$$f = \frac{1}{N} \sum_{n=1}^N g_i(E, T - T_{\text{base}}) \Sigma_x(E'_n, T_{\text{base}}). \quad (19)$$

As  $N$  approaches infinity, the value of the response approaches to

$$\iint g_i(E, T - T_{\text{base}}) \Sigma_x(v', T_{\text{base}}) \times \frac{1}{g_i(E, T - T_{\text{base}})} \frac{v'}{2v} \times P_{\text{MB}}(V_t, T - T_{\text{base}}) d\mu dV_t = \Sigma_x(v, T) = \Sigma_x(E, T), \quad (20)$$

i.e. the effective cross section at temperature  $T$ . In Eq. (20), the normalized form of the target velocity distribution (10) has been used (Viitanen and Leppänen, 2014). This approach increases the CPU time spent in the sampling of the cross sections as the target velocities need to be resampled in case  $N > 1$ . Therefore, the total number of samples  $N$  should be optimized for the best performance.

Even though the temperature difference between the material and  $T_{\text{base}}$ , and usage of TMS in general, increases the variances of the scores, it also affects the number of collisions in the transport: An increase in the temperature difference  $T_{\text{max}} - T_{\text{base}}$  decreases the sampling efficiency of the rejection sampling criterion (14), which increases the proportion of rejected or “virtual” collisions in the transport. Consequently, the collision estimators are scored more often than in an ordinary calculation with the same number of neutron histories, which has a decreasing effect on the variances of estimators. It is, hence, not self-evident whether the total effect of TMS on the variances of collision estimators is increasing or decreasing.

### 3.4. Figures-of-merit

What comes to the calculation of reaction rates, it is, in practice, not the amount of statistics obtained per transported neutron but the amount of statistics per spent CPU time that counts. The best quantity to describe the overall performance of a Monte Carlo code in reaction rate estimation is the figure-of-merit, defined

$$\text{FOM} = \frac{1}{\tau \sigma^2}, \quad (21)$$

where  $\tau$  is the calculation time and  $\sigma^2$  is the variance of an estimator. Since the variance is, by theory, inversely proportional to  $\tau$ , the value of FOM should be independent of the total calculation time. Thus, it describes purely the efficiency of the calculational system in the calculation of reaction rates. The higher the FOM, the better the performance.

The usage of the TMS temperature treatment has effect on both parameters  $\tau$  and  $\sigma$ . The effect of TMS on  $\sigma$  has been previously described. When it comes to  $\tau$ , it has been examined in Viitanen and Leppänen (2012a, 2013, 2014) that the calculation time required per transported neutron is somewhat higher with the TMS method than with methods relying on effective cross sections. After introduction of reaction rate estimators with the stochastic scoring scheme, the calculational overhead may increase further. Since the usage of TMS increases both  $\sigma$  and  $\tau$ , it is expected that the figures-of-merit are somewhat worse with the TMS than with conventional transport methods.

## 4. Test cases

The performance of the TMS method in reaction rate estimation is tested in four systems with different neutron spectra to provide an overall picture of its performance in practice. The test cases are the same as in Viitanen and Leppänen (2014).

### 4.1. Gd-doped pressurized water reactor assembly (PWR-Gd)

The first “PWR-Gd” case involves a  $17 \times 17$  PWR fuel assembly with 16 Gadolinium-doped fuel rods in an infinite two dimensional lattice. The geometry and material definitions of the fuel assembly are from an NEA benchmark (Roque et al., 2004). The only differences to the benchmark specifications are related to temperatures: the moderator temperature is risen to 600 K for simplicity and the originally flat temperature profiles of the fuel rods are replaced with 3-step distributions such that the pellets are divided into three equi-thick annular regions with temperatures 600, 900, and 1200 K from outside in.

In the PWR-Gd case, the estimators are scored in the fuel material of the four corner rods.

### 4.2. PWR-Gd assembly at 40 MWd/kgU burnup (PWR-BU)

The second case is abbreviated “PWR-BU” and features the previously introduced “PWR-Gd” bundle irradiated to 40 MWd/kgU burnup. The irradiated material compositions were obtained by running a separate burnup calculation using Serpent 2.1.14. The resulting compositions contain 241 actinide and fission product nuclides with cross sections available in the data libraries.

The estimators are scored in the fuel material of the four corner rods also in the PWR-BU case.

### 4.3. High temperature gas cooled reactor system (HTGR)

The “HTGR” test case consists of TRISO particles within graphite matrix in an infinite three dimensional lattice. The specifications of the TRISO particles and the composition of the graphite matrix are based on a NEA benchmark for HTGR fuel depletion (DeHart and Ulses, 2009), and the lattice pitch is 0.16341 cm. The fuel kernel in the spherical TRISO particles is divided in two equally thick parts such that the innermost 0.0125 cm is at 1800 K temperature and the outer layer is at 1200 K. The temperature of all other materials is 1200 K.

The estimators in the HTGR case are scored in all of the fuel material.

### 4.4. Sodium cooled fast reactor assembly (SFR)

The last of the test cases, “SFR”, involves a fuel assembly from the sodium cooled fast reactor JOYO in an infinite two dimensional lattice. The specifications of the assembly can be found in Nuclear Energy Agency (2006). The geometry and material definitions correspond to the benchmark definition for the 250 °C core. Again, the fuel temperature is modified such that the inner half (radius) of the fuel pellets is at 1200 K and the outer half at 900 K temperature. All other materials are at 600 K temperature in the model.

In the SFR case, the estimators are scored in the fuel material of all 6 corner rods of the hexagonal fuel assembly.

## 5. Results

The results are calculated using a development version of Serpent, which is based on Serpent 2.1.14. The cross section library used in the calculations is JEFF-3.1.1 based and it has been processed with NJOY 99.364 using a rather low 0.001 reconstruction tolerance (MacFarlane and Muir, 2000). TMS treatment is used for fuel materials only, and all the other materials are modeled using NJOY-broadened cross sections. In the reference calculations, pre-broadened cross sections are used also for the fuel materials.

The Serpent transport routine is optimized for performance using pre-generated material-wise total cross sections to avoid summation over material compositions during tracking

(Leppänen, 2009). This method results in a considerable speed-up in calculation, especially when modeling irradiated fuels. The same optimization cannot, however, be used together with the TMS method. Thus, comparing the performance of a typical Serpent calculation to a calculation with the TMS treatment would be somewhat misleading. To provide for fair comparison of the transport methods, the material-wise total cross sections were omitted also from all performance-related reference calculations by running Serpent in optimization mode 2, which has been originally developed for Serpent 2 for the purpose of saving memory in large burnup calculations (Leppänen and Isotalo, 2012).

Since the TMS method is not capable of correctly modeling the unresolved resonances, the energy region of unresolved resonances is handled using infinitely dilute cross sections without any special treatment in all of the calculations. Doppler-broadening rejection correction is used for  $^{238}\text{U}$  between 0.4 eV and 20 keV in all of the thermal systems. Because of the recent findings in Viitanen and Leppänen (2014), the use of DBRC was extended in the PWR-BU case to nuclides  $^{95}\text{Mo}$ ,  $^{108}\text{Pd}$ ,  $^{131}\text{Xe}$ ,  $^{145}\text{Nd}$ ,  $^{147}\text{Pm}$ ,  $^{152}\text{Sm}$ ,  $^{239}\text{Pu}$ ,  $^{240}\text{Pu}$ ,  $^{242}\text{Pu}$  and  $^{241}\text{Am}$  in addition to  $^{238}\text{U}$ . To be precise, DBRC was used only in the reference calculations and TMS calculations with Elevated Basis Temperatures. When using TMS with 0 K basis cross sections the temperature dependence of the elastic scattering kernel is inherently taken into account (Viitanen and Leppänen, 2014).

All the calculations are made using 12 OpenMP threads on a 3.47 GHz Intel Xeon X5690 processor. The results were normalized to  $10^{15}$  total flux in all of the cases.

### 5.1. Comparison of reaction rates

The very first thing to do is to ensure that the collision estimators provide, on average, the same results with the TMS method as with conventional tracking methods. This is done by comparing the

total reaction rate and capture rate spectra of TMS calculations to reference solutions based on NJOY broadened cross sections. The spectra are scored using 1000 equi-lethargy bins from  $10^{-11}$  to 20 MeV and the calculations are performed using two variations of the TMS method: in the “TMS/0 K” variant,  $T_{\text{base}}$  equals 0 Kelvin, while the “TMS/EBT” (Elevated Basis Temperature) variant involves basis cross sections at the minimum temperature of each nuclide. The parameters and integral results of these calculations are provided in Table 1.

Because of the similarity of the results, the differences in the total reaction rate and capture rate spectra are provided here only for the HTGR case, which has the best statistics for the whole energy spectrum. In Figs. 1 and 2 it can be seen that the estimator results correspond to the reference solution within statistical accuracy at all energies. Also the integral results presented in Table 1 are in perfect agreement.

The performance measures in Table 1 show that the TMS/EBT method performs very well when calculating energy-integrated reaction rates: the figures-of-merit are practically equal to the reference in two out of four cases, namely in the PWR-Gd and HTGR cases. In the PWR-BU case, about twice the CPU time is required by the TMS/EBT method to obtain the same statistical deviation as in the reference calculation, since sampling the velocities of all 241 nuclides at each collision site takes a lot of calculational effort. In the SFR case the TMS method, a little surprisingly, outperforms the reference. This is due to the fact that the optimization mode 2 of Serpent uses a multi-group delta-tracking majorant cross section in the neutron tracking, which slows down the calculation especially at high neutron energies when compared to the TMS method with a continuous-energy majorant.

The figures-of-merit are much worse with TMS/0 K. For example, to obtain a certain level of statistical accuracy in the most inefficient PWR-BU case, about 12 times more CPU time is required than in a conventional Monte Carlo transport calculation.

**Table 1**

Integral results and performance measures for the reference solution and two variants of the TMS method in four test cases. The “rel.” values in the TMS results are calculated relative to the NJOY based reference solution.

	PWR-Gd	PWR-BU	HTGR	SFR
Number of active neutron histories	$10^9$	$5 \times 10^7$	$5 \times 10^8$	$10^9$
<i>NJOY based reference</i>				
Transport time (h)	7.14	2.27	10.39	15.30
Memory requirement (GB)	2.59	77.45	0.72	1.92
Tot. reaction rate ( $\frac{1}{s}$ )	2.036E+12	2.020E+12	1.074E+13	1.004E+13
$\sigma$ (%)	0.014	0.062	0.002	0.003
Capture rate ( $\frac{1}{s}$ )	1.245E+11	1.931E+11	1.672E+12	1.601E+11
$\sigma$ (%)	0.029	0.109	0.004	0.005
Tot. reaction rate, FOM ( $\frac{1}{s}$ )	2.0E+03	3.2E+02	6.7E+04	2.0E+04
Capture rate, FOM ( $\frac{1}{s}$ )	4.6E+02	1.0E+02	1.7E+04	7.3E+03
<i>TMS/EBT</i>				
Transport time, tot./rel. (h/-)	7.13/1.00	4.50/1.98	10.41/1.00	10.31/0.67
Memory requirement tot./rel. (GB/-)	1.89/0.73	33.44/0.43	0.72/1.00	1.64/0.86
Tot. reaction rate ( $\frac{1}{s}$ )	2.036E+12	2.014E+12	1.074E+13	1.004E+13
$\sigma$ (%)	0.014	0.062	0.002	0.003
Capture rate ( $\frac{1}{s}$ )	1.245E+11	1.927E+11	1.672E+12	1.601E+11
$\sigma$ (%)	0.028	0.108	0.004	0.005
Tot. reaction rate, FOM, tot./rel. ( $\frac{1}{s}$ /-)	2.0E+03/1.00	1.6E+02/0.50	6.7E+04/1.00	3.0E+04/1.48
Capture rate, FOM, tot./rel. ( $\frac{1}{s}$ /-)	5.0E+02/1.07	5.3E+01/0.51	1.7E+04/1.00	1.1E+04/1.49
<i>TMS/0 K</i>				
Transport time, tot./rel. (h/-)	17.81/2.50	25.93/11.42	25.63/2.47	16.24/1.06
Memory requirement tot./rel. (GB/-)	1.98/0.76	40.73/0.53	0.76/1.00	2.42/1.26
Tot. reaction rate ( $\frac{1}{s}$ )	2.036E+12	2.019E+12	1.073E+13	1.004E+13
$\sigma$ (%)	0.014	0.061	0.002	0.003
Capture rate ( $\frac{1}{s}$ )	1.245E+11	1.929E+11	1.672E+12	1.600E+11
$\sigma$ (%)	0.029	0.111	0.005	0.005
Tot. reaction rate, FOM, tot./rel. ( $\frac{1}{s}$ /-)	8.0E+02/0.40	2.9E+01/0.09	2.7E+04/0.41	1.9E+04/0.94
Capture rate, FOM, tot./rel. ( $\frac{1}{s}$ /-)	1.8E+02/0.40	8.7E+00/0.08	4.3E+03/0.26	6.8E+03/0.94

Please cite this article in press as: Viitanen, T., Leppänen, J. Effect of the Target Motion Sampling temperature treatment method on the statistics and performance. Ann. Nucl. Energy (2014), <http://dx.doi.org/10.1016/j.anucene.2014.08.033>

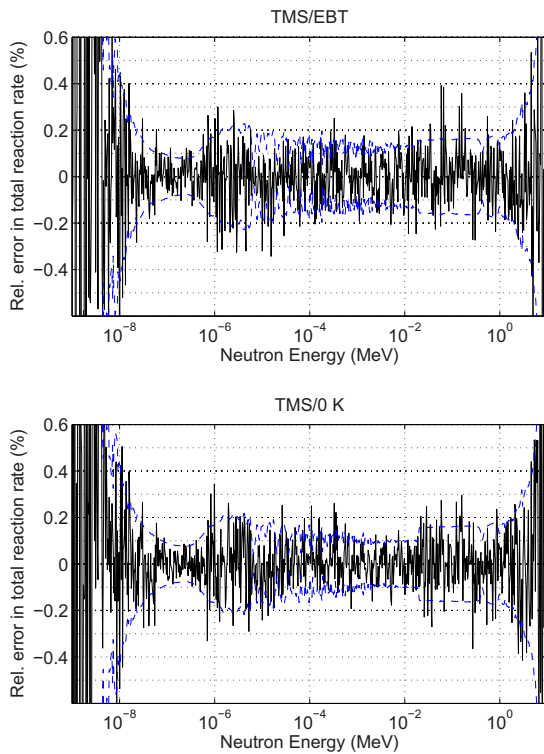


Fig. 1. Differences in total reaction rate spectra compared to an NJOY based reference solution. Results are provided for TMS with two different basis cross section temperatures. The dashed line represents one-sigma standard deviation.

In many cases it is, however, not the energy-integrated reaction rate, but the contribution of a smaller energy region that is of interest. The energy dependence of the variances is examined in the next section.

## 5.2. Variance spectra

Serpent was run for each of the four test cases with number of resampling,  $N$ , ranging from 1 to 100 using 5 million active neutron histories. Again, the calculations were made using two different basis temperatures. For comparison purposes, the results of an NJOY based reference calculation are also provided.

The effect of the response resampling on variances is first examined through the standard deviations of the total reaction rate and capture rate spectra. Since the results are, again, quite similar for all of the test cases, only the results of the PWR-BU test case are provided. Selected results are depicted in Figs. 3–7. The results calculated with 0 K basis are provided mainly to emphasize the effects of the TMS technique on variances: the results in the previous section suggest that EBT variant should always be used for the best performance.

It should also be noted that the plots in Figs. 3–7 represent the statistical deviations, not the figures-of-merit. As can be seen in Table 1, the  $N = 1$  calculation with TMS/0 K takes about 11.5 times more calculation time than the reference calculation and changing the  $N$  parameter increases the calculation time further by about 10% with  $N = 10$  or about 140% with  $N = 100$  in the PWR-BU case. Thus, even though it seems that the statistical deviations become

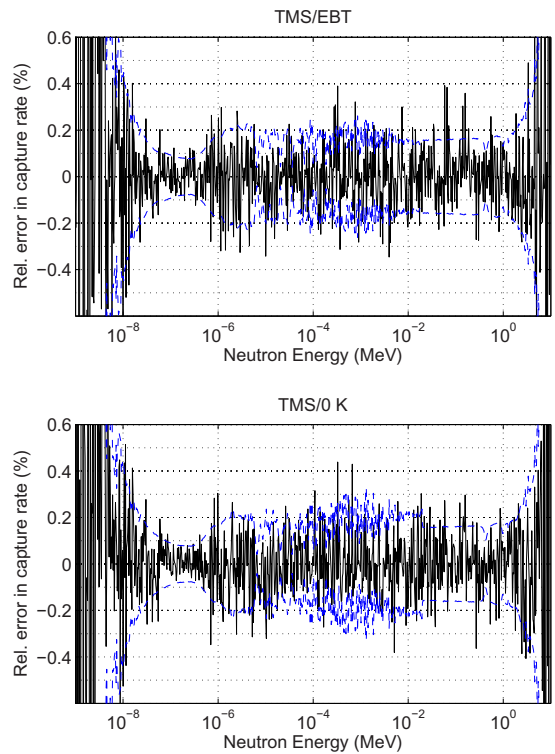


Fig. 2. Differences in capture rate spectra compared to an NJOY based reference solution.

slightly smaller with TMS/0 K than with the reference, the figures-of-merit are in fact much worse. With TMS/EBT the calculational overhead to reference is much smaller and, hence, the figures-of-merit would be much closer but still worse than the reference.

Several conclusions can be drawn based on these results:

- In Fig. 3 it can be seen that resampling does not have significant effect on the variances when calculating the total reaction rate. It can also be seen that around  $10^{-3}$  MeV, for instance, the TMS method with 0 K basis results in smaller variances than a conventional calculation with the same number of neutron histories, apparently due to an increase in the number of virtual collisions because of the lowered rejection sampling efficiency. The standard deviation curves are connected above  $2 \times 10^{-2}$  MeV, which corresponds to the lower boundary of the energy region of unresolved resonances for  $^{238}\text{U}$ .
- The advantages of resampling can be recognized in Fig. 4, between energies  $2 \times 10^{-4}$  and  $2 \times 10^{-2}$  MeV. The increasing of  $N$  decreases the variance of the capture rate estimator. With sufficiently high values of  $N$  the standard deviation is approximately halved, decreasing it even below that of the reference calculation. It also seems that at this energy region already a few additional samples decreases the variance of the estimator significantly. Since both the total reaction rate and capture rate estimators are scored equally often, the differences in estimator variances can only be explained by the fact that the total cross section is relatively smooth compared to the capture cross section.

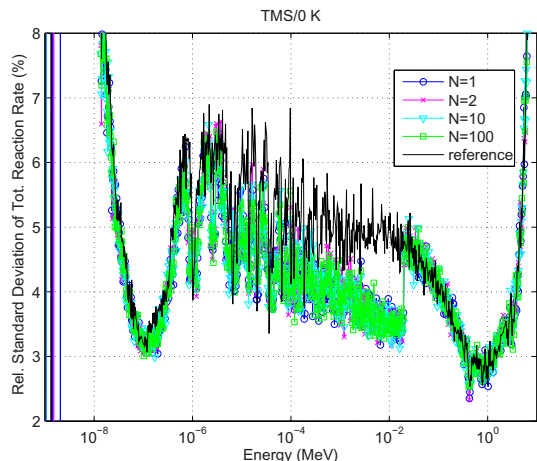


Fig. 3. Relative standard deviations of the total reaction rate spectra for the PWR-BU case. The TMS calculations with different numbers of responses  $N$  are done using basis cross sections at 0 K. The reference solution is based on NJOY-broadened cross sections.

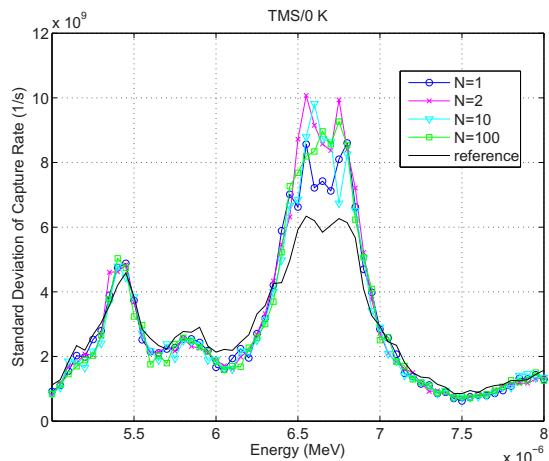


Fig. 5. A selected detail in the capture rate deviation spectrum of the PWR-BU case, calculated using TMS/0 K: the surroundings of the 6.7 eV resonance peak of  $^{238}\text{U}$ .

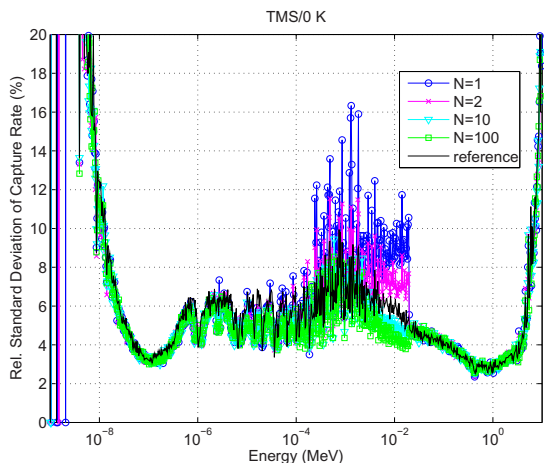


Fig. 4. Relative standard deviations of the capture rate spectra for the PWR-BU case. Zero Kelvin basis cross sections are used in the TMS calculations.

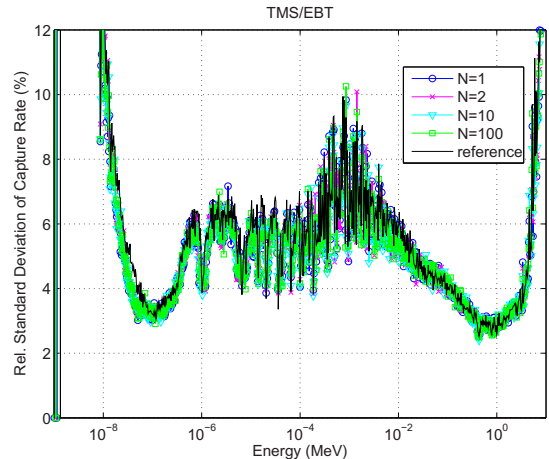


Fig. 6. Relative standard deviations of the capture rate spectra for the PWR-BU case. The TMS calculations are made using elevated basis cross section temperatures (EBT).

- The behavior around the 6.7 eV resonance of  $^{238}\text{U}$  in Fig. 5 shows that around very strong resonances the variances in the capture rate are larger than the reference in all calculations with TMS. In fact, it was noticed that with TMS also the statistical deviation of the neutron flux around the strongest resonances is somewhat higher than in an ordinary calculation with effective cross sections, which implies that this behavior is not related to the usage of distributed responses.
- The results in Figs. 6 and 7 show that when using TMS with EBT the value of  $N$  does not affect the standard deviations at any energy region, in practice. The issue around the strong resonances exists also with EBT, but the standard deviations of the TMS calculations are slightly closer to the reference than in the 0 K cases.

The fact that the quality of the response samples is only important at a particular energy region seems to be related to the energy range of the effect of thermal motion, which according to Eq. (7) is directly proportional to the square root of neutron energy. Since the spacing and average width of the resonances are roughly constant (at least in magnitude) throughout the whole energy spectrum, the broadening of the extent of thermal motion means that the energy region from which the response values are sampled contains a higher number of resonances and the probability of hitting an individual resonance is much smaller than at low energies. This increases significantly the variances of responses, which is also reflected in the estimator results. It should be noted that the energy range defined by Eq. (7) depends also on the mass of the nuclide and the temperature. Hence, the phenomenon is emphasized for light resonance absorber nuclides at high temperatures.

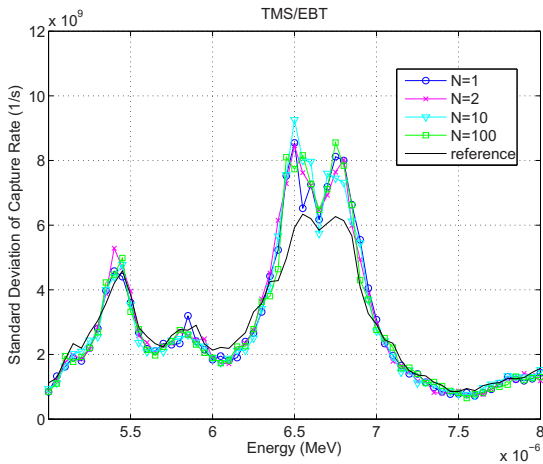


Fig. 7. A selected detail in the capture rate deviation spectrum of the PWR-BU case, calculated using TMS/EBT: the surroundings of the 6.7 eV resonance.

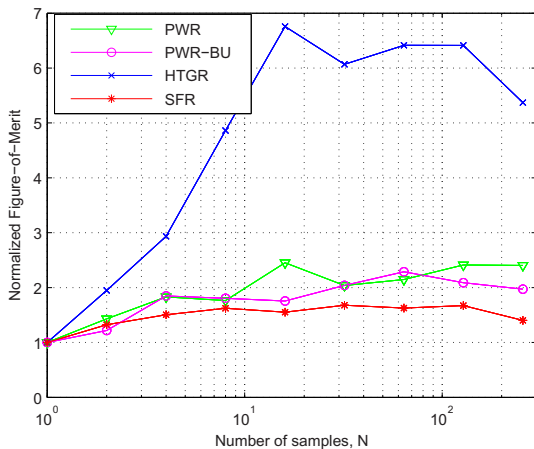


Fig. 8. Normalized figures-of-merit of reaction rate estimators in four test cases, scored using averages of  $N = 1 - 256$  response samples. The estimators are scored between 2–4 keV.

### 5.3. Effect of resampling

In the previous, it was noticed that increasing of the  $N$  parameter has a decreasing effect on the variance of the total capture rate between energies  $2 \times 10^{-4}$  and  $2 \times 10^{-2}$  MeV, but only when using TMS/O K. To examine the corresponding effect on the figures-of-merit, the capture reaction rate between 2–4 keV was estimated with different values of  $N$ . Five million active neutron histories were run per each calculation. The results are depicted in Fig. 8.

When resampling is applied only at a narrow energy interval, the value of  $N$  has only minor effect on the calculation times. Changing  $N$  from 1 to 256 increased the overall calculation time by 64% in the HTGR case, while the extra calculation time was less than 12% in all other cases. The figures-of-merit in Fig. 8 show that the performance of the TMS method in high-energy reaction rate estimation can be significantly increased using the resampling method. With optimal number of samples  $N$  the figure-of-merit

Table 2

Figures-of-merit for a capture rate estimator scored around the 6.7 eV resonance of  $^{238}\text{U}$ .

	PWR		PWR-BU		HTGR	
	Abs.	Rel.	Abs.	Rel.	Abs.	Rel.
NJOY Based Reference	1.08E+03	1.00	8.66E+01	1.00	1.23E+05	1.00
TMS/EBT	5.09E+02	0.47	3.49E+01	0.40	6.71E+04	0.54
TMS/O K	2.12E+02	0.20	6.14E+00	0.07	2.75E+04	0.22

can be increased even by a factor of six in the HTGR case and by a factor of about 1.5–2 in other systems.

### 5.4. Figures-of-merit near strong resonances

To express the importance of the previously-discovered effect around strong resonances also in terms of figures-of-merit, the capture rate around the 6.7 eV resonance of  $^{238}\text{U}$  was calculated using a single energy bin between 6.5–6.9 eV. The results for the thermal systems are provided in Table 2.

The figures-of-merit for TMS/O K are in any case significantly smaller than for reference because of longer calculation times, but those for TMS/EBT should, in general, be very close to the reference in the light of the previous results. Hence, based on the TMS/EBT results in Table 2 it can be concluded that the whole 50% decrease in figures-of-merit around strong resonances is caused by the newly-found behavior.

According to the current understanding, the behavior is caused by a relative increase in TMS score variances in case of highly probable reactions. When considering a constant number of neutron histories, the usage of TMS usually decreases the variances because TMS transport adds virtual collisions, at which the collision estimators are scored, along the neutron tracks. Specifically, this effect adds virtual collisions also for such neutrons that do not experience any actual collisions within a material region in which the estimators are scored. Since a couple of scores from virtual collisions is much better for the statistics than no scores at all, the use of TMS in many cases decreases the estimator variances.

However, the situation becomes a little different at energies where the cross sections are very high and, correspondingly, the mean free paths are very small. Near strong resonances the probability of a neutron to experience a real collision is near 100% and, therefore, it is very likely to get one collision estimator score out of each neutron track in the material zone of interest even with conventional tracking methods. It turns out that individual scores corresponding to the actual collisions (conventional transport) result in smaller estimator variances than sums of  $n$  scores corresponding to the numerous virtual collisions along the way to the reaction site (TMS), since  $n$  is in fact a random variable. Consequently, the TMS method results in slightly poorer estimator statistics near strong resonances and there is, in practice, nothing to do about it. Hopefully, a more rigorous description of the phenomenon will be provided in the future.

## 6. Summary and conclusions

In this work, the effect of the TMS temperature treatment method on the performance of total reaction rate and capture rate estimators has been studied. Because of a limitation in the geometry routine of the Serpent Monte Carlo code, the study was, at this point, limited to collision estimators only. To better understand the effect of distributed cross section responses on the variances of the estimators, a resampling technique was introduced to decrease the response variances. This technique is simply based on using an

average of  $N$  response samples instead of an individual value in the estimator scoring.

The reaction rate results calculated using the TMS method agreed with the NJOY based reference solution within statistical accuracy throughout the energy spectrum. By examining closely the deviance spectra calculated using the response resampling technique with different values for  $N$ , it was noticed that the usage of sampled response function values only had practical effect on the estimator variances when scoring the capture rate estimator at energies between  $2 \times 10^{-4}$  and  $2 \times 10^{-2}$  MeV and the effect was only present when TMS method was used with 0 Kelvin cross sections. With elevated basis temperatures (EBT) or with total reaction rate estimators the “quality” of the responses had no effect on the estimator variances.

The only energy region in which the TMS with EBT performed notably worse than the reference was near very strong resonances: in the vicinity of resonances the statistical deviations of all estimators, including the flux estimator, increased above the reference. This behavior decreased the figures-of-merit near very strong resonances by about 50% compared to the reference, while the performance was practically equal further away from the strong resonances. The effect is, according to current knowledge, caused by the fact that the summing over a random number of scores from virtual collisions results in higher estimator variances than usage of individual scores from actual collisions if the probability of a neutron to experience an actual collision is very high.

It seems that the usage of sampled response values has much smaller effect on the variances of estimators than anticipated beforehand by the authors. In those cases, where the usage of sampled responses significantly deteriorated the variances of the estimators, the performance could be effectively boosted using the response resampling technique. However, it should be noted that in the current study these cases were always associated with the usage of TMS with 0 Kelvin basis temperatures. In practical calculations, the EBT version will be always used and, thus, the resampling will be futile.

In summary, the TMS method with EBT seems to perform very well in the calculation of reaction rates and the performance seems to be governed by the efficiency of the neutron tracking. It is, however, possible that new issues would emerge if more exotic materials and reactions would be investigated: this study was only limited to the behavior of total reaction rate and capture rate estimators in typical fuel materials. The applicability of the method

with track length estimators is considered a very important topic and is to be examined in the near future.

## Acknowledgements

This work is partly funded through the NUMPS project of the Finnish Academy and KÄÄRME project of the Finnish Research Programme on Nuclear Power Plant Safety, SAFIR2014.

## References

- Becker, B., Dagan, R., Lohnert, G., 2009. Proof and implementation of the stochastic formula for ideal gas, energy dependent scattering kernel. *Ann. Nucl. Energy* 36, 470–474.
- DeHart, M.D., Ulses, A.P., 2009. Benchmark specification for HTGR fuel element depletion. Tech. Rep. NEA/NSC/DOC(2009)13, Nuclear Energy Agency.
- Leppänen, J., 2009. Two practical methods for unionized energy grid construction in continuous-energy Monte Carlo neutron transport calculation. *Ann. Nucl. Energy* 36, 878–885.
- Leppänen, J., 2010. Performance of Woodcock delta-tracking in lattice physics applications using the Serpent Monte Carlo reactor physics burnup calculation code. *Ann. Nucl. Energy* 37, 715–722.
- Leppänen, J., Isotalo, A., 2012. Burnup calculation methodology in the Serpent 2 Monte Carlo code. In: *PHYSOR-2012*. Knoxville, TN, Apr. 15–20, 2012.
- Lux, I., Koblinger, L., 1990. *Monte Carlo Particle Transport Methods: Neutron and Photon Calculations*. CRC Press, Boca Raton, Florida.
- MacFarlane, R.E., Muir, D.W., 2000. NJOY99.0 code system for producing pointwise and multigroup neutron and photon cross sections from ENDF/B data. Tech. Rep. PSR-480, Los Alamos National Laboratory.
- Nuclear Energy Agency, 2006. Japan's experimental fast reactor Joyo Mk-I core: sodium-cooled uranium-plutonium mixed oxide fueled fast core surrounded by UO<sub>2</sub> blanket, international handbook of evaluated reactor physics benchmark experiments. Tech. Rep. NEA/NSC/DOC(2006)1, Nuclear Energy Agency.
- Ogibin, V., Orlov, A., 1984. Majorized cross-section method for tracking neutrons in moving media. *Voprosy Atomnoj Nauki i Tekhniki, Metodiki i Programmy* 2 (16), 6–9, in Russian.
- Roque, B., et al., 2004. Specification for the phase 1 of a depletion calculation benchmark devoted to fuel cycles. Tech. Rep. NEA/NSC/DOC(2004)11, Nuclear Energy Agency.
- Viitanen, T., Leppänen, J., 2012a. Explicit temperature treatment in Monte Carlo neutron tracking routines – first results. In: *PHYSOR-2012*. Knoxville, TN, Apr. 15–20, 2012.
- Viitanen, T., Leppänen, J., 2012b. Explicit treatment of thermal motion in continuous-energy Monte Carlo tracking routines. *Nucl. Sci. Eng.* 171, 165–173.
- Viitanen, T., Leppänen, J., 2013. Optimizing the implementation of the explicit treatment of thermal motion – how fast can it get? In: *M&C 2013*. Sun Valley, ID, May 5–9, 2013.
- Viitanen, T., Leppänen, J., 2014. Target motion sampling temperature treatment technique with elevated basis cross section temperatures. *Nucl. Sci. Eng.* 177, 77–89.
- X-5 Monte Carlo Team, 2003. MCNP—a general Monte Carlo n-particle transport code, version 5. Tech. Rep. LA-UR-03-1987, Los Alamos National Laboratory.